Hindawi Publishing Corporation
Advances in Materials Science and Engineering
Volume 2016, Article ID 5317985, 5 pages
http://dx.doi.org/10.1155/2016/5317985

Research Article

Stress Coupling Effect on Ideal Shear Strength: Tungsten as a Case Study

Miroslav Černý, Petr Šesták, and Jaroslav Pokluda

Central European Institute of Technology (CEITEC), Brno University of Technology (VUT), Purkyňova 123, 612 00 Brno, Czech Republic

Correspondence should be addressed to Miroslav Černý; cerny.m@fme.vutbr.cz

Received 19 September 2016; Revised 10 November 2016; Accepted 14 November 2016

Academic Editor: Rui Wang

Copyright © 2016 Miroslav Černý et al. This is an open access article distributed under the Creative Commons Attribution License, which permits unrestricted use, distribution, and reproduction in any medium, provided the original work is properly cited.

Mechanical response of a perfect bcc tungsten crystal to a multiaxial loading was investigated from first principles. The multiaxial stress state consisted of the shear stress and a superimposed compressive triaxial stress with various levels of differential stresses. The studied shear system was ⟨111⟩{110}. Results obtained within a relatively wide range of the compressive stresses showed that increasing hydrostatic triaxial stress (with zero differential stresses) increased the shear strength almost linearly. On the other hand, triaxial stresses with greater portion of the differential components did not have such a simple effect on the shear strength: we found a certain optimum value of the superimposed triaxial stress yielding the maximum shear strength. Any change (both increase and decrease) in the triaxial stress then reduced the ideal shear strength value.

1. Introduction

First-principles (ab initio) approaches have proven useful and reliable not only in chemistry and condensed matter physics [1, 2] but also in many other scientific areas including materials science [3, 4]. For this reason, they are routinely employed in simulations of deformation processes, predictions of limits of stability and strength, studies of inherent properties of crystals, and so forth [3, 5, 6]. There is no doubt that there are problems that are beyond the reach of these methods such as interactions of defects in crystal lattice (requiring very large computational cells due to periodic boundary conditions) or the effect of temperature. Attempts to overcome computational difficulties related to avoiding some of the approximations embedded in the ab initio methods have not yielded any efficient and generally accepted solution so far. On the other hand, there are many research problems that cannot be solved using available experimental tools and the ab initio methods then represent the only way to obtain reliable data.

Typically, investigation of the stress-strain response of a crystal lattice far from its equilibrium is experimentally hardly accessible. The major reason is a presence of lattice defects that reduce the attainable level of mechanical stresses by several orders of magnitude in comparison with the ideal strength [7]. As a consequence, the strains that can be applied to the crystal lattice are also remarkably lowered due to structure relaxation by movement and interactions of the defects. Fortunately, the computational approaches based on quantum mechanics are able to supply results that are equally reliable both close to the crystal equilibrium and far from it. A lot of computational effort has therefore been invested into mapping the limits of strength and stability of solid crystals. Although real material samples always contain certain amount of defects, properties of ideal crystal can serve as important input parameters in various multiscale models of complex deformation processes. Moreover, modern experimental equipment makes it possible to approach limits of strength in several specific cases such as the tensile testing of nanowhiskers [8], compression of nanopillars [9], or nanoindentation testing [10] of well-prepared samples.

The major problem is thus not obtaining the data but their interpretation. Relatively high computational demands of these methods not only impose serious limitations on the size of the simulation cell mentioned above but also motivate researchers to make their simulations relatively simple to keep the computational time within acceptable limits. In the particular case of ideal (theoretical) strength, the

models usually try to mimic ideally uniaxial loading [11–13] or simple shear [14, 15]. Unfortunately, in majority of real situations, crystal loading is very different from the simple stress states considered in such calculations. Several examples of theoretical studies on multiaxial loading are, however, also available (see, e.g., the review [6] and the references therein).

In the present paper, our attention will be paid to a multiaxial stress state described as a combination of shear and normal stresses. Such a stress state occurs, for example, under the nanoindenter tip. Former studies [16–18] suggested that the shear strength of many metals can be raised by superposition of a compressive stress acting normal to the shear planes. Recently, we reported remarkable difference in the responses of shear strength of bcc tungsten crystal to normal stresses when two distinct cases of the superimposed stresses, the uniaxial and the isotropic stresses, were considered [6]. Here we intend to describe the effect of triaxiality of the superimposed stress on the ideal shear strength in a more detailed way.

2. Computational Details

In the present study, the crystal is subjected to a superposition of the shear stress τ and the three normal stresses σ_1, σ_2, and σ_3 illustrated in Figure 1. Although directions of the arrows in Figure 1 correspond to tensile normal stresses, the stresses considered in our study are mostly compressive. For the sake of simplicity, the superimposed normal stresses fulfill the relation

$$\sigma_1 = \sigma_2 = \lambda\sigma_3, \tag{1}$$

where the compressive stress σ_3 oriented perpendicular to the shear planes pushes the shear planes closer to each other. From now on, this stress will be denoted (consistent with our former studies) σ_n. The other two stresses σ_1 and σ_2 correspond to normal in-plane stresses that stretch or shrink the shear planes. According to (1), differential stresses linearly decrease with increasing λ. The parameter λ can also be used to express the stress triaxiality and its values 0 and 1 are associated with the purely uniaxial and the isotropic (hydrostatic) loadings, respectively. Stress triaxiality factor T, which is usually defined by the ratio of hydrostatic stress to the equivalent von Mises stress, can be expressed in terms of λ:

$$T = \frac{1 + 2\lambda}{3\,(1 - \lambda)}. \tag{2}$$

In our study, however, we prefer describing the stress state using λ over using T, value of which is infinity for hydrostatic stress. The stress state (superimposed to the shear) is thus described using the parameters σ_n and λ and the ideal shear strength can be calculated as their function.

The investigated shear system in the bcc W crystal is one of the $\langle 111\rangle\{110\}$ ensemble. Directions of the arrows in Figure 1, representing σ_1, σ_2, and σ_3 (σ_n), can thus be parallel, for example, to the respective $[11\bar{2}]$, $[111]$, and $[1\bar{1}0]$ crystallographic directions.

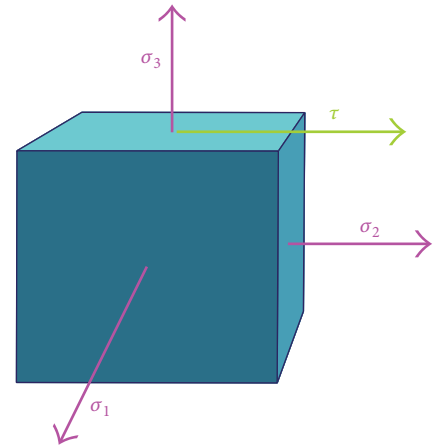

Figure 1: The model of multiaxial loading composed of the shear stress τ and normal stresses σ_1, σ_2, and σ_3.

For the first-principles calculations of the stress tensor, we employed the Abinit code [19, 20], a common project of the Université Catholique de Louvain, Corning Incorporated, and other contributors (URL http://www.abinit.org/). The valence electrons were described using the ultrasoft pseudopotential. The exchange-correlation contribution to the energy was evaluated by means of the generalized gradient approximation with the parametrization by Perdew et al. [21]. The cut-off energy was set to 400 eV and the mesh of $23 \times 23 \times 23$ k-points was used for sampling over the Brillouin zone. The self-consistent cycle was finished after the total energy was converged within 10^{-7} eV. The crystal was partially relaxed using our external program for optimization of the cell shape (to converge the controlled stress tensor components to the predetermined values with allowed deviations below 0.15 GPa). Namely, all the components of the resulting stress tensor

$$\begin{bmatrix} \lambda\sigma_n & 0 & 0 \\ 0 & \lambda\sigma_n & \tau \\ 0 & \tau & \sigma_n \end{bmatrix} \tag{3}$$

were controlled with the only exception of the shear stress τ whose value was calculated for set of shear strains in order to find its maximum. The stress tensor was taken directly from the output of the Abinit code [22]. As a benchmark, we evaluated the stress also from finite differences of the total energy (computed as a function of the axial strain). The agreement was very good (within the considered computational error of 10^{-1} GPa).

3. Results and Discussion

The very first step in any simulation of crystal deformation is always an optimization of the structure and finding its ground state. This way we obtained the stress-free bcc W crystal with the lattice parameter of 3.17 Å which agrees well with the measured value of 3.16 Å [23]. Also the computed bulk modulus of 317 GPa is close to the experimental value of

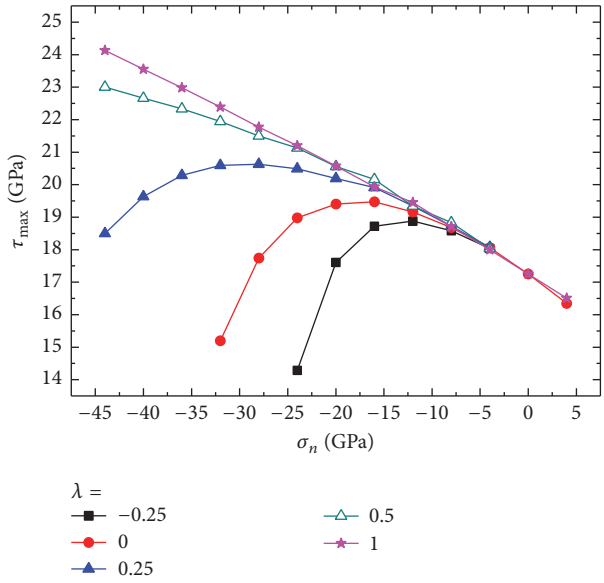

FIGURE 2: The ideal shear strength τ_{max} as a function of the superimposed normal stress σ_n for several values of the parameter λ.

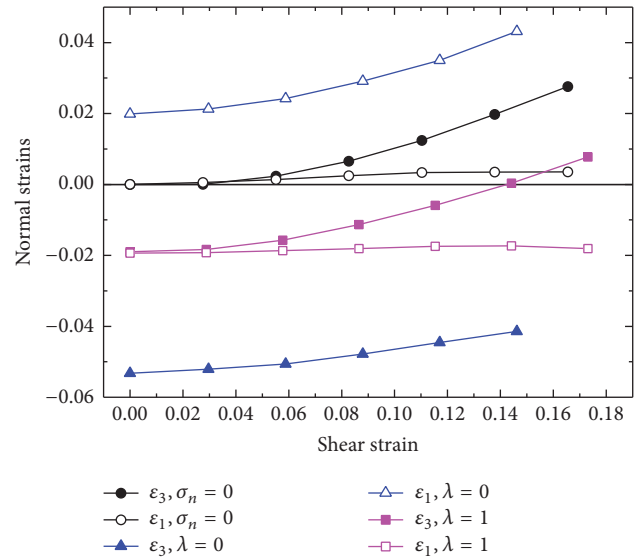

FIGURE 3: Evolution of the normal strains ε_1 (open symbols) and ε_3 (solid symbols) in the W crystal during shear straining. The circles illustrate evolution of the strains during the pure shear. The squares and triangles display the data points corresponding to superimposed hydrostatic and uniaxial stresses of −20 GPa, respectively.

310 GPa [23]. Then we applied a simple shear (i.e., for $\sigma_n = 0$) and calculated the shear stress maximum $\tau_{max,0}$. Its value of 17.3 GPa was in a good agreement with the ideal shear strength value of 17.5 GPa computed by Ogata et al. [14].

The same shear procedure was then employed to calculate the shear strength τ_{max} for several values of σ_n and for five different values of the parameter λ ranging from −0.25 to 1. The results are displayed in Figure 2 in terms of $\tau_{max}(\sigma_n)$ dependencies, each corresponding to a different value of λ.

As can be seen, the responses of τ_{max} to the normal stress strongly depend on the parameter λ. When the triaxial stress state is isotropic ($\lambda = 1$), the shear strength steadily increases with increasing compressive σ_n. The displayed dependence can be approximated by a linear function $\tau_{max} = \tau_{max,0} + k\sigma_n$, where $k = -0.16$ expresses the slope of the linear fit. Reducing λ results in noticeable bending of $\tau_{max}(\sigma_n)$ dependence. The superimposed stresses then increase the ideal shear strength only within a certain range of σ_n and, after reaching an optimum σ_n value corresponding to the maximum value of τ_{max}, further increase in σ_n rapidly reduces the shear strength. When the superimposed stress is uniaxial ($\lambda = 0$), the optimum σ_n value is approximately equal to −19 GPa. The corresponding data points are almost identical with those reported formerly [18], though the present results were obtained using somewhat different computational settings. We also tried to combine the normal compression with a transverse tension (with corresponding value $\lambda = -0.25$) which reduced the optimum value of σ_n to about −13 GPa. As far as we know, the limited number of studies focused on the effect of normal stresses on the shear strength (e.g., [16–18]) considered mostly the stress state corresponding to $\lambda = 0$. Comparing the present results for tungsten with those computed earlier for other bcc metals [18], one can see a very similar response obtained for Mo crystal. $\tau_{max}(\sigma_n)$ dependencies calculated for crystals of Fe, Ta, or Nb were almost linear in the whole range of investigated stresses. Within a limited range of normal stresses in similar studies devoted to ⟨111⟩{112} shear system in bcc crystals [17], $\tau_{max}(\sigma_n)$ dependencies computed for the same group of elements were qualitatively the same, that is, almost linear.

Differences in computed $\tau_{max}(\sigma_n)$ curves for different values of λ can be easily understood from the crystal behavior during shear straining. Shifting neighboring planes requires the atoms to overcome an energy barrier. Corresponding τ_{max} value is proportional to the height of the barrier which depends, besides other things, on a distance between the shear planes and a distance of atoms measured in the plane perpendicular to the shear direction. There is no doubt that the larger these distances are, the lower the barrier is. Thus the crystal can respond to a shear deformation by an increase of the related normal strains. Figure 3 displays the normal strains ε_1 and ε_3 (corresponding to directions of the stresses in Figure 1) as functions of the shear strain (up to the strain value corresponding to τ_{max}). Data for a pure shear ($\sigma_n = 0$) show that the values of ε_3 grow more rapidly than those of ε_1, which means that the crystal prefers expanding perpendicular to the shear planes (increasing interplanar distance) over extending the planes.

To illustrate the effect of λ on structural relaxation of the W crystal, we extended Figure 3 by the data for superimposed normal stresses of the magnitude $\sigma_n = -20$ GPa. For clarity, the figure only contains strains computed for the hydrostatic ($\lambda = 1$) and uniaxial ($\lambda = 0$) superimposed stresses. Results for the hydrostatic stress show that crystal relaxes practically the same way as during a pure shear except that the curves for both strains are shifted by about −0.02 since the crystal is isotropically compressed. Such a constraint must

substantially raise both the energy barrier and τ_{max}. Uniaxial stress, however, changes the crystal relaxation during shearing remarkably: the strain ε_1 increases more rapidly (even more than ε_3) which means that the Poisson expansion in this direction facilitates the shear process by reducing the energy barrier (as well as τ_{max}) in comparison with the case of hydrostatic stress.

This result is not very surprising. It has, however, important consequences for construction of multiscale models of deformation processes. For example, models intended for interpretation of nanoindentation data must consider triaxiality of the stress state very carefully since the normal stresses occurring in critical microvolumes where the resolved shear stress reaches the ideal shear strength can be very high. For example, Zhu et al. [24] evaluated the stress state in their nanoindentation model for Cu and obtained a triaxial stress above 8 GPa and the shear strength of about 4.6 GPa. For tungsten these values are, of course, higher exceeding 30 GPa for normal stresses. In such a case, τ_{max} values computed under uniaxial and hydrostatic normal stresses differ by more than 30% and the difference rapidly increases with increasing σ_n (as can be seen from Figure 2). Fortunately, the data in Figure 2 also show that results computed for superimposed stress states with λ above 0.5 and those for the hydrostatic stress state are very similar. Thus, in certain cases, multiscale models assuming only the hydrostatic superimposed stresses (as, e.g., the recent nanoindentation model [25]) can supply reliable predictions even if the real stress state slightly deviates from the assumption. Nevertheless, considering the appropriate stress state in multiscale models of deformation processes is crucial for guaranteeing correctness of the results.

4. Conclusions

Theoretical shear strength of the bcc tungsten was computed from first principles as a function of the superimposed triaxial compressive stress. The results revealed that the effect of the superimposed stresses on the shear strength depends not only on the magnitude of the stresses but also on their triaxiality. Nearly isotropic stress states raise the shear strength almost linearly with increasing normal stress magnitude, whereas the stress states with greater differential stresses have the increasing effect only up to a certain "optimum" stress magnitude, exceeding which leads to the right opposite effect. The optimum level of superimposed normal stresses was found decreasing with increasing magnitude of differential stresses. These results are very important for future utilization of ab initio data in multiscale models of deformation processes since correct description of the stress state is one of the key steps in evaluation of results.

Competing Interests

The authors declare that they have no competing interests.

Acknowledgments

The authors acknowledge the financial support by the Ministry of Education, Youth and Sports of the Czech Republic under the Project CEITEC 2020 (Project no. LQ1601).

References

[1] I. Turek, V. Drchal, J. Kudrnovský, M. Šob, and P. Weinberger, *Electronic Structure of Disordered Alloys, Surfaces and Interfaces*, Springer, Berlin, Germany, 1997.

[2] S. Elliot, *The Physics and Chemistry of Solids*, John Wiley & Sons, New York, NY, USA, 2005.

[3] J. Pokluda and P. Šandera, "Micromechanisms of fracture and fatigue," in *Multiscale Context*, Springer, London, UK, 2010.

[4] R. Dronskowski, *Computational Chemistry of Solid State Materials*, Wiley, New York, NY, USA, 2005.

[5] G. Grimvall, B. Magyari-Köpe, V. Ozoliņš, and K. A. Persson, "Lattice instabilities in metallic elements," *Reviews of Modern Physics*, vol. 84, no. 2, pp. 945–986, 2012.

[6] J. Pokluda, M. Černý, M. Šob, and Y. Umeno, "Ab initio calculations of mechanical properties: methods and applications," *Progress in Materials Science*, vol. 73, pp. 127–158, 2015.

[7] N. H. Macmillan, "The theoretical strength of solids," *Journal of Materials Science*, vol. 7, no. 2, pp. 239–254, 1972.

[8] G. Richter, K. Hillerich, D. S. Gianola, R. Mönig, O. Kraft, and C. A. Volkert, "Ultrahigh strength single crystalline nanowhiskers grown by physical vapor deposition," *Nano Letters*, vol. 9, no. 8, pp. 3048–3052, 2009.

[9] J. M. Wheeler, R. Raghavan, J. Wehrs, Y. Zhang, R. Erni, and J. Michler, "Approaching the limits of strength: measuring the uniaxial compressive strength of diamond at small scales," *Nano Letters*, vol. 16, no. 1, pp. 812–816, 2016.

[10] J. Li, K. J. Van Vliet, T. Zhu, S. Yip, and S. Suresh, "Atomistic mechanisms governing elastic limit and incipient plasticity in crystals," *Nature*, vol. 418, no. 6895, pp. 307–310, 2002.

[11] W. Luo, D. Roundy, M. L. Cohen, and J. W. Morris, "Ideal strength of bcc molybdenum and niobium," *Physical Review B*, vol. 66, no. 9, Article ID 094110, 2002.

[12] R. H. Telling, C. J. Pickard, M. C. Payne, and J. E. Field, "Theoretical strength and cleavage of diamond," *Physical Review Letters*, vol. 84, no. 22, pp. 5160–5163, 2000.

[13] M. Černý, M. Šob, J. Pokluda, and P. Šandera, "*Ab initio* calculations of ideal tensile strength and mechanical stability in copper," *Journal of Physics Condensed Matter*, vol. 16, no. 7, pp. 1045–1052, 2004.

[14] S. Ogata, J. Li, N. Hirosaki, Y. Shibutani, and S. Yip, "Ideal shear strain of metals and ceramics," *Physical Review B*, vol. 70, no. 10, Article ID 104104, 2004.

[15] D. M. Clatterbuck, D. C. Chrzan, and J. W. Morris Jr., "The ideal strength of iron in tension and shear," *Acta Materialia*, vol. 51, no. 8, pp. 2271–2283, 2003.

[16] A. Kelly, W. R. Tyson, and A. H. Cottrell, "Ductile and brittle crystals," *Philosophical Magazine*, vol. 15, no. 153, pp. 567–581, 1967.

[17] M. Černý, P. Šesták, and J. Pokluda, "Influence of superimposed normal stress on shear strength of perfect bcc crystals," *Computational Materials Science*, vol. 47, no. 4, pp. 907–910, 2010.

[18] M. Černý, P. Šesták, and J. Pokluda, "Strength of bcc crystals under combined shear and axial loading from first principles," *Computational Materials Science*, vol. 55, pp. 337–343, 2012.

[19] X. Gonze, J.-M. Beuken, R. Caracas et al., "First-principles computation of material properties: the ABINIT software project," *Computational Materials Science*, vol. 25, no. 3, pp. 478–492, 2002.

[20] X. Gonze, B. Amadon, P.-M. Anglade et al., "ABINIT: first-principles approach to material and nanosystem properties,"

Computer Physics Communications, vol. 180, no. 12, pp. 2582–2615, 2009.

[21] J. P. Perdew, K. Burke, and M. Ernzerhof, "Generalized gradient approximation made simple," *Physical Review Letters*, vol. 77, no. 18, pp. 3865–3868, 1996.

[22] M. Torrent, F. Jollet, F. Bottin, G. Zérah, and X. Gonze, "Implementation of the projector augmented-wave method in the ABINIT code: application to the study of iron under pressure," *Computational Materials Science*, vol. 42, no. 2, pp. 337–351, 2008.

[23] D. R. Lide, *Handbook of Chemistry and Physics*, CRC Press, Boca Raton, Fla, USA, 86th edition, 2005.

[24] T. Zhu, J. Li, K. J. Van Vliet, S. Ogata, S. Yip, and S. Suresh, "Predictive modeling of nanoindentation-induced homogeneous dislocation nucleation in copper," *Journal of the Mechanics and Physics of Solids*, vol. 52, no. 3, pp. 691–724, 2004.

[25] P. Šandera, J. Pokluda, T. Schöberl, J. Horníková, and M. Černý, "Modeling Load-displacement Curve and Pop-in Effect in Nanoindentation Tests," *Procedia Materials Science*, vol. 3, pp. 1111–1116, 2014.


Journal of
Nanotechnology

International Journal of
Corrosion

International Journal of
Polymer Science

Smart Materials
Research

Journal of
Composites

BioMed
Research International
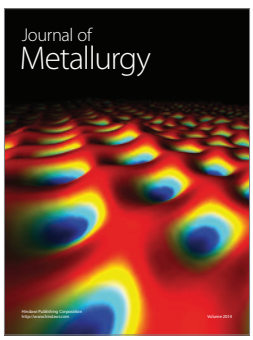
Journal of
Metallurgy

Journal of
Materials

Hindawi
Submit your manuscripts at
http://www.hindawi.com
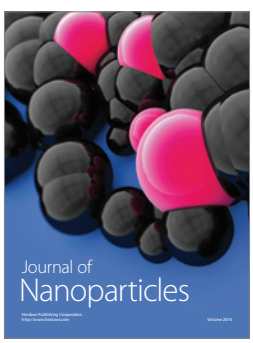
Journal of
Nanoparticles
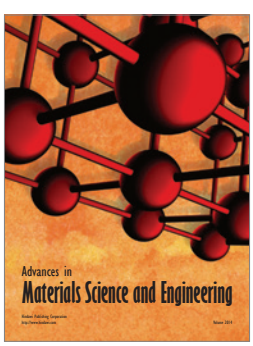
Advances in
Materials Science and Engineering
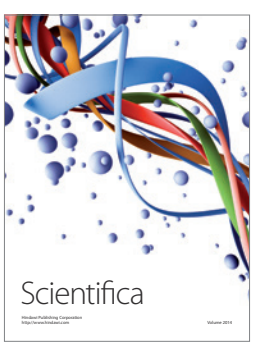
Scientifica
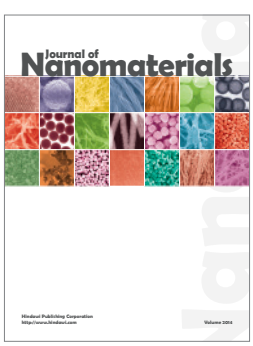
Journal of
Nanomaterials

The Scientific
World Journal

International Journal of
Biomaterials
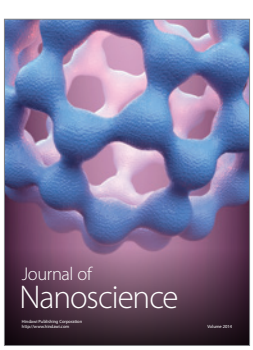
Journal of
Nanoscience

Journal of
Coatings
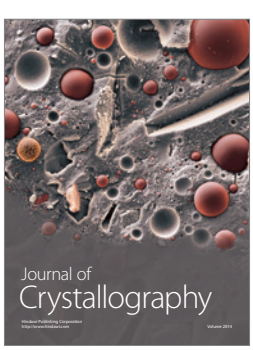
Journal of
Crystallography

Journal of
Ceramics
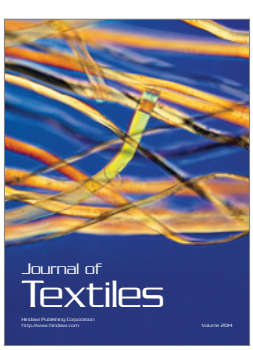
Journal of
Textiles